J. Membrane Biol. 79, 75–86 (1984)

The Journal of
Membrane Biology

Thermotropic Lipid Phase Separations in Human Erythrocyte Ghosts and Cholesterol-Enriched Rat Liver Plasma Membranes

Larry M. Gordon* and Patrick W. Mobley†

*Rees-Stealy Research Foundation, San Diego, California 92101, and †Department of Chemistry, California State Polytechnic University, Pomona, California 91768

Summary. Electron spin resonance (ESR) studies of human erythrocyte ghosts labeled with 5-nitroxide stearate, I(12,3), indicate that a temperature-dependent lipid phase separation occurs with a high onset at 38°C. Cooling below 38°C induces I(12,3) clustering. Similar phase separations were previously identified in human platelet and cholesterol-loaded [cholesterol/phospholipid molar ratio (C/P) = 0.85] rat liver plasma membranes [L.M. Gordon et al., 1983; *J. Membrane Biol.* **76;** 139–149]; these were attributed to redistribution of endogenous lipid components such that I(12,3) is excluded from cholesterol-rich domains and tends to reside in cholesterol-poor domains. Further enrichment of rat liver plasma membranes to C/P ratios of 0.94–0.98 creates an "artificial" system equivalent to human erythrocyte ghosts (C/P = 0.90), using such criteria as probe flexibility, temperature dependent I(12,3) clustering; and polarity of the probe environment. Consequently, cholesterol-rich and -poor domains probably exist in both erythrocyte ghosts and high cholesterol liver membranes at physiologic temperatures. The temperature dependence of cold-induced hypertonic lysis of intact human erythrocytes was examined by incubating cells in 0.9 M sucrose for 10 min at 1°C intervals between 9 and 46°C (Stage 1), and then subjecting them to 0°C for 10 min (Stage 2). Plots of released hemoglobin are approx. sigmoidal, with no lysis below 18°C and maximal lysis above 40°C. The protective effect of low temperatures during Stage 1 may be due to the formation of cholesterol-rich domains that alter the bilayer distribution and/or conformation of critical membrane-associated proteins.

Key Words erythrocyte ghosts · liver plasma membranes · spin probe · cholesterol · lipid phase separation · lipid domains · hemolysis

Introduction

Convincing evidence indicates that discrete lipid domains exist in erythrocyte plasma membranes. For example, phospholipids are asymmetrically arranged about the outer and inner leaflets, with negatively-charged lipids predominating in the cytosol half of the bilayer [34]. Distinct clusters of phosphatidylserine and phosphatidylethanolamine have been detected with the use of cross-linking agents [31]. Moreover, separate pools of phosphatidylcholine [41] were identified using phospholipases as hydrolyzing agents. Another important constituent, the neutral lipid cholesterol, is inhomogeneously distributed [1, 12, 24]. Nonrandom lipid ordering may be responsible for those restricted lipid domains previously identified in erythrocyte membranes [44].

Since membrane lipids associate on the basis of weak, noncovalent interactions (e.g., hydrophobic and electrostatic), physical properties of erythrocyte lipid domains are probably sensitive to temperature changes. Indeed, temperature-dependent lipid phase transitions (or separations) have been reported in the range 11–41°C using a variety of physical-biochemical techniques [5, 6, 13, 14, 23, 35, 43, 45, 47, 48]. Considerable uncertainty remains, however, concerning the exact nature of those lipid domains participating in the above melting phenomena.

Here, the thermotropic lipid phase separation in human erythrocyte ghosts is investigated by studying the temperature-dependent flexibility and clustering of the 5-nitroxide stearate spin probe, I(12,3)[1]. To test whether cholesterol content is an important modulator of thermotropic lipid phase separations in high-cholesterol membranes, we similarly examine rat liver plasma membranes enriched

[1] *Abbreviations used:* I(12,3), the N-oxyl-4′,4′-dimethyloxazolidine derivative of 5′-ketostearic acid; DSC, differential scanning calorimetry; ESR, electron spin resonance; I(5,10), the N-oxyl-4′,4′-dimethyloxazolidine derivative of 12′-ketostearic acid; I(10,3), the N-oxyl-4′,4′-dimethyloxazolidine derivative of 5′-ketopalmitic acid; NMR, nuclear magnetic resonance; C/P, the cholesterol/phospholipid molar ratio; **L**, liquid lipid domains; **QCC**, quasicrystalline cluster lipid domains; **S**, solid lipid domains; CIHL, cold-induced hypertonic lysis of erythrocytes.

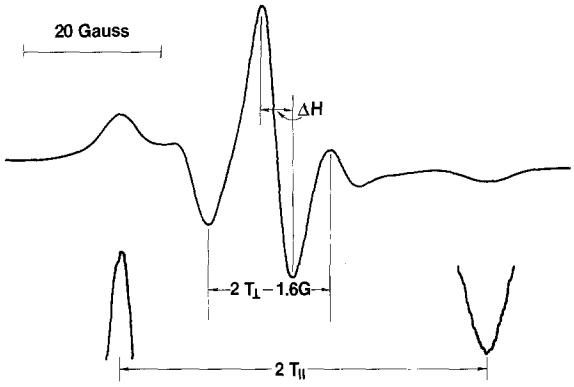

Fig. 1. ESR spectrum of I(12,3)-labeled human erythrocyte ghosts at 37°C, recorded using a Varian E-104A spectrometer with a 4-min scan time, 5×10^4 receiver gain, 2 G modulation amplitude and 0.5 sec time-constant. Outer peaks were magnified by recording at 5×10^5 receiver gain and 16-min scan time. The outer and inner hyperfine splittings, $2T_{\parallel}$ and $2T_{\perp}$, were measured as shown; $2T_{\perp}$ was corrected by the addition of 1.6 G [21]. The peak-to-peak linewidth of the central line in the spectrum (ΔH) is indicated. The μg probe/mg membrane protein ratio was 3.3

with cholesterol to C/P ratios approximating those of human erythrocytes (i.e., C/P ~ 0.9).

Materials and Methods

Materials

The I(12,3) spin probe was obtained from Syva Co., Palo Alto, CA. All other chemicals and reagents were from Sigma Chemical Co., St. Louis, MO.

Preparation of Human Erythrocyte Ghosts and Cholesterol-Enriched Rat Liver Plasma Membranes

Ghosts were prepared from intact human erythrocytes [37]. Cholesterol enrichment of purified rat liver plasma membranes was performed by incubation with cholesterol-rich liposomes; cholesterol and phospholipid determinations were as set out earlier [46].

Membrane Spin-Labeling and Spectral Recording

Methods for ESR studies were as described previously [7, 20, 21]. For spin-label studies, human erythrocyte ghosts and rat liver plasma membranes were suspended in 50 mM triethanolamine-HCl, 8% (wt/vol) sucrose, pH 7.4 at 4 mg protein/ml. Samples were used fresh or after storage at −70°C. Membrane incorporation of I(12,3) and spectral recording were as set out earlier [20]. The spin label/membrane ratios used were: (i) 3.3 to 30 μg I(12,3) per mg of erythrocyte protein (or 1 probe per 144 − 16 lipid); (ii) 2.5 to 27 μg I(12,3) per mg protein of native [C/P = 0.71] liver membranes (or 1 probe per 104 − 10 lipid); and (iii) 2.5 to 27 μg I(12,3) per mg protein of cholesterol-enriched [C/P = 0.94–0.98] liver membranes (or 1 probe per 115 − 11 lipid). Probe/lipid was calculated assuming all lipid to be phospholipid and cholesterol. Figure 1 shows the ESR spectrum of I(12,3)-labeled human erythrocyte ghosts.

Evaluation of the Flexibility of the Membrane-Incorporated I(12,3) Probe

The following order parameter expressions [19] may be used to evaluate the flexibility of the fatty acid spin probe:

$$S(T_{\parallel}) = 1/2\left[\frac{3(T_{\parallel} - T_{xx})}{(T_{zz} - T_{xx})} - 1\right] \quad (1)$$

$$S(T_{\perp}) = 1/2\left[\frac{3[(T_{zz} + T_{xx}) - 2T_{\perp}]}{(T_{zz} - T_{xx})} - 1\right] \quad (2)$$

$$S = \frac{(T_{\parallel} - T_{\perp})(a_N)}{(T_{zz} - T_{xx})(a_N')}. \quad (3)$$

$T_{\parallel}$ and $T_{\perp}$ for the membrane-incorporated probe are the hyperfine splitting elements parallel and perpendicular to z', the symmetry axis of the effective Hamiltonian (**H'**), while T_{xx} and T_{zz} are the hyperfine splitting elements of the static interaction tensor (**T**) parallel to the static Hamiltonian (**H**) principal nuclear hyperfine axes x and z. Elements of **T** were determined by incorporating nitroxide derivatives into host crystals: $(T_{xx}, T_{zz}) = (6.1, 32.4)$ G [7] a_N' and a_N are the isotropic hyperfine coupling constants for probe in membrane crystal [i.e., $a_N' = 1/3(T_{\parallel} + 2T_{\perp})$ and $a_N = 1/3(T_{zz} + 2T_{xx})$]. Increases in a_N' reflect a more polar environment.

If experimentally-determined low probe concentrations are employed [36], S, $S(T_{\parallel})$ and $S(T_{\perp})$ are sensitive to membrane fluidity (or, more accurately, the flexibility of the incorporated probe). S, $S(T_{\parallel})$ and $S(T_{\perp})$ may each assume values between 0 and 1, with the extreme limits indicating that the probe samples fluid and immobilized environments. S, which requires both hyperfine splittings, corrects for small polarity differences between membrane and reference crystal. Although $S(T_{\parallel})$ and $S(T_{\perp})$ do not include polarity corrections, these expressions are useful fluidity approximations [19].

Determination of Nitroxide Radical Interactions

Estimation of probe-probe interactions [7, 20, 36] in I(12,3)-labeled human erythrocyte ghost and rat liver plasma membranes was performed as follows. The first index of radical interactions involves determining the peak-to-peak linewidth of the central line (i.e., ΔH of Fig. 1)

$$\Delta H = \Delta H_o + \Delta H_{dip} + \Delta H_{ex} \quad (4)$$

where ΔH_o is the linewidth without interactions, ΔH_{dip} is the line broadening caused by magnetic dipolar interactions and ΔH_{ex} is contributed by spin-spin exchange [7]. Enhanced probe-probe interactions increase ΔH. The second measure is based on the observation that $T_{\perp}$, but not $T_{\parallel}$, broadens with increasing probe concentration in various membranes [7, 8, 36]. Consequently, for those probe concentrations where the percent change in $S(T_{\parallel})$,

$\Delta S(T_\parallel)$, is zero, decreases in $S(T_\perp)$ with increasing probe concentration reflect enhanced I(12,3) clustering.

Measurement of Cold-Induced Hypertonic Lysis (CIHL)

Cold-induced hypertonic lysis of human erythrocytes was studied following the protocol of Green and Jung [22], with several modifications. Freshly-obtained erythrocytes were washed three times in 0.85% NaCl, and packed cells from the last wash were used to make a 2% erythrocyte suspension in a hypertonic medium, consisting of 0.877 M sucrose, 5 mM Tris-HCL, pH 7.25. 25 μl of packed erythrocytes were added to a 1.5-ml conical, plastic microfuge tube containing 1.3 ml of hypertonic medium. Tube and solution had been earlier equilibrated in a well at the desired temperature (*see* below) and were returned to this well after cell addition and vortexing. Time out of the well was always less than 20 sec. After 10 min of this Stage 1 incubation, tubes were removed, vortexed, and immediately placed in a water-ice slurry at 0°C. After incubating for 10 min (Stage 2), tubes were removed, vortexed, and placed in a gently-shaking room temperature (*RT*) bath until centrifuged. The treated erythrocyte suspension was centrifuged in a Beckman microfuge B for 1.5 min at *RT*. Supernatant solution was withdrawn and its absorbance at 543 nm measured. Percent lysis was calculated, using as reference the average of three tubes in which 25 μl of packed cells were incubated in 1.3 ml of distilled water for the duration of the experiment.

The dependence of CIHL on Stage 1 temperature (9–46°C) was examined using an Arrhenius block device. As configured in our laboratory, the main body of the block is a solid piece of aluminum alloy 6061, with dimensions of 0.70 × 0.05 × 0.05 m. At each end of the block, a perpendicular extension with the same dimensions of the main body projects downward 0.15 m. Along the top of the U-shaped block at evenly-spaced intervals (5 mm), 42 pairs of wells were drilled to accommodate 1.5 ml plastic microfuge tubes. The well depth was approx. the length of the microfuge tube, while its diameter was slightly less than that of the microfuge tube. This allows the tube to fit snugly in the well, while providing room beneath for a temperature-equilibrated water reservoir. The block was placed with one leg in a high temperature bath (GCA Precision Scientific Tempstir, 12 liter capacity) at 56°C and the other in a low temperature bath (Exacal Constant Temperature Bath Circulator, Neslab) at 5°C. All exposed block faces were covered with styrofoam, and 1 hr was allowed for temperature equilibration. Well temperatures were measured with a Tektronix digital thermometer. The Arrhenius block sets up a stable, linear temperature gradient (9–46°C), permitting rapid measurement of the effects on CIHL of varying Stage 1 temperature in 1.0 ± 0.1°C intervals. This device has been used to assess enzyme activities in the range 0–42°C [25] and 25–47°C [17].

Results and Discussion

The Effects of I(12,3) Concentration on the Order Parameters and ΔH of Human Erythrocyte Ghost Membranes

Figure 1 is the ESR spectrum of erythrocyte ghosts labeled with a low I(12,3) concentration, and shows

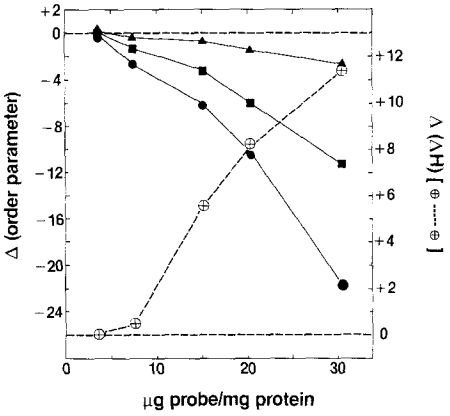

Fig. 2. Probe concentration effects on order parameters and ΔH of I(12,3)-labeled human erythrocyte ghosts at 30°C. $\Delta S(T_\parallel)$ [▲], $\Delta S(T_\perp)$ [●], and ΔS [■] are percent changes from baseline values measured at 4.0 μg I(12,3)/mg protein. Control $S(T_\parallel)$, $S(T_\perp)$ and S were 0.768, 0.594 and 0.665. $\Delta(\Delta H)$ [⊕---⊕] is percent change in ΔH from the baseline value of 5.25 G

that the incorporated probe undergoes rapid anisotropic motion about its long molecular axis at physiologic temperatures. Raising the probe/mg membrane protein ratio, by addition of I(12,3), decreased the high-field peak of the inner hyperfine doublet, displaced downward the high-field baseline and upward the low-field base-line, increased $2T_\perp$ and ΔH, and left $2T_\parallel$ unchanged. Similar spectral alterations occurred with $I(12,3)$-labeled whole human erythrocytes [3].

As the probe concentration was increased, S and $S(T_\perp)$ decreased substantially, while $S(T_\parallel)$ remained essentially constant (Fig. 2). These order parameter effects are most likely attributed to enhanced probe-probe interactions and are not due to membrane fluidization. The broadening of $T_\perp$ [and decrease in $S(T_\perp)$] was closely correlated with increases in ΔH (Fig. 2); earlier investigations have shown that radical interactions broaden the ΔH of labeled model and biological membranes [7, 36]. Reductions in S and $S(T_\perp)$ were also associated with such characteristic exchange-broadening effects as the decrease in the high-field peak height of the inner hyperfine doublet and the downward displacement of the high-field baseline (*see* Fig. 2 in Gordon et al. [20]). The finding that $T_\parallel$ [and $S(T_\parallel)$] is essentially unaltered for erythrocyte membranes (Fig. 2) indicates that the "apparent" increase in fluidity with probe concentration, denoted by reductions in S and $S(T_\perp)$, is not the result of probe-mediated membrane perturbations; any fluidization that permits more probe flexibility requires that $T_\parallel$ decrease commensurately with increases in $2T_\perp$ and that ΔH narrows. Similar $I(m,n)$ concentration effects on

order parameters have been observed in many other biological membranes [7, 38].

Nitroxide radical interactions are absent for I(12,3) concentrations less than approx. 5 μg probe/mg protein at 30°C (Fig. 2). Thus, the S, $S(T_\parallel)$ and $S(T_\perp)$ control values of Fig. 2 reflect "intrinsic" or "magnetically-dilute" order parameters [36].

It is improbable that the probe effects in Fig. 2 are due to increased dipole interactions, but rather are the result of enhanced spin-exchange arising from I(12,3) clustering. This is because the probe undergoes rapid anisotropic motion at 30°C and dipole-dipole interactions are relatively long range, tending to be averaged out by rapid diffusion and/or tumbling while exchange interactions require that labels be in van der Waal's contact and decrease rapidly with distance.

Temperature-Dependence of the Order Parameters of I(12,3)-Labeled Human Erythrocyte Ghosts

For erythrocyte ghost membranes labeled with a low probe concentration, Arrhenius-type plots of S, $S(T_\parallel)$ and $S(T_\perp)$ (Fig. 3*A*) show that temperature reductions increased each order parameter. Figure 3*A* also indicates that the slopes of the order parameter *vs.* $1/T$(°K) curves become steeper in the following order: $S(T_\perp) < S < S(T_\parallel)$. No "breaks" characteristic of thermotropic lipid phase separations were readily apparent. However, low probe range $S(T_\perp)$ and S could not be measured below 15°C due to slow probe motion and poorly-resolved inner hyperfine doublets.

Temperature effects on the order parameters were also examined with erythrocyte membranes labeled with a high I(12,3) concentration (Fig. 3*A*). The $S(T_\parallel)$ *vs.* $1/T$(°K) curves using either low or high probe concentrations were in excellent agreement. However, high range S and $S(T_\perp)$ values were considerably less than corresponding low range order parameters for each temperature in the range 40–22°C. Δ (order parameter) *vs.* $1/T$(°K) plots were calculated as the percent difference between values obtained at "high" and "low" probe concentrations. Figure 3*B* indicates that $\Delta S(T_\perp)$ and ΔS become increasingly more negative below approx. 38°C, while $\Delta S(T_\parallel)$ did not significantly vary from zero. The invariance of $S(T_\parallel)$ suggests that, for "low" and "high" probe concentrations, ESR spectra reflect only those I(12,3) that sample lipid domains sharing the same fluidity and polarity. Since it is reasonable to assume that the flexibility and polarity contributions to "low" and "high" range $S(T_\parallel)$ will be equal at a given temperature [7], $\Delta S(T_\perp)$ [or, alternatively, $\Delta T_\perp$] is here an empirical parameter reflecting only radical interactions. It should be recalled that $S(T_\perp)$ decreased as the I(12,3) concentration increased in erythrocyte membranes at 30°C, while $S(T_\parallel)$ remained unchanged (Fig. 2). The observation that $\Delta S(T_\perp)$ in Fig. 3*B* becomes more negative below 38°C therefore suggests that cooling also promotes probe-probe interactions in human erythrocyte membranes.

These findings are consistent with earlier studies of spin-labeled mammalian surface membranes. For temperatures less than 37, 32 or 28°C in human platelet, rat heart, or rat liver plasma membranes, respectively, Arrhenius-type plots of Δ (order parameters) indicated increased spin exchange interactions due to I(12,3) clustering [17, 20].

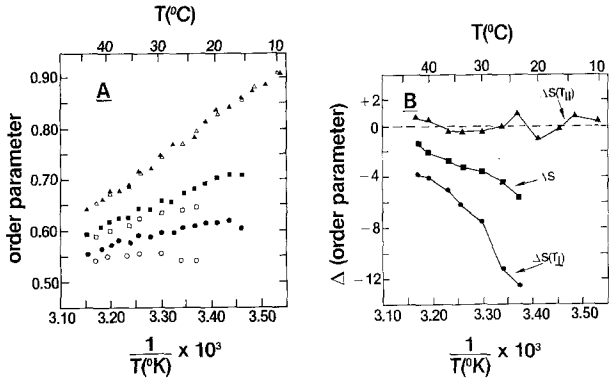

Fig. 3. Temperature dependence of the order parameters of I(12,3)-labeled human erythrocyte ghosts. (*A*): $S(T_\parallel)$ [▲], S [■] and $S(T_\perp)$ [●] were measured using a "low" probe concentration (i.e., 4μg probe/mg protein), while $S(T_\parallel)$ [△], S [□] and $S(T_\perp)$ [○] were obtained with a "high" probe concentration (i.e., 20 μg probe/mg protein). (*B*): Δ (order parameter) was the percent difference between values measured at the "high" and "low" probe concentrations of *A*

Temperature Dependence of the Order Parameters of I(12,3)-Labeled Cholesterol-Enriched Rat Liver Plasma Membranes

For cholesterol-enriched liver plasma membranes [C/P = 0.96 ± 0.02, mean ± SD, number of preparations = 3] labeled with a low I(12,3) concentration, Arrhenius plots of $S(T_\parallel)$ indicated "breaks" or "discontinuities" at approx. 37 and 18°C (Fig. 4). This suggests that a broad lipid phase separation occurs between these temperatures that perturbs I(12,3) flexibility. Order parameter *vs.* $1/T$(°K) plots were also determined for low and high probe load-

ing (Fig. 5*A*). Although $S(T_{\parallel})$ of membranes labeled with either low or high I(12,3) concentrations were in good agreement, high-range S and $S(T_{\perp})$ values were much below those of membranes labeled with a low probe concentration (Fig. 5*A*). As Arrhenius-type plots of Δ (order parameter) indicate that $S(T_{\perp})$ declines for temperatures less than approx. 38°C, while $S(T_{\parallel})$ remains unchanged (Fig. 5*B*), we believe that cooling below the 37–38°C onset sequesters I(12,3).

The above thermotropic lipid phase separation may be compared with those identified in native [C/P = 0.71] and cholesterol-enriched [C/P = 0.85] rat liver plasma membranes [17, 18, 20]. Using low probe concentrations, Arrhenius-type plots of order parameters demonstrated breaks at 28 and 19°C, suggesting that a lipid phase separation in native membranes perturbs I(12,3) flexibility [17, 36]. Furthermore, Arrhenius-type plots of Δ (order parameters) indicated I(12,3) segregation below 28°C [17, 20]. For reasons discussed earlier [20], we proposed a model in which solid (**S**) and liquid (**L**) lipid domains coexist below 19°C. The 19°C break corresponds to **S** and **L** being dispersed into "quasicrystalline" clusters (**QCC**) and **L**. Here, **QCC** are defined as having a packing density and fluidity between that of **S** and **L**. **QCC** decreases with heating above 19°C until the 28°C transition is reached and remaining **QCC** are converted into **L**. Consequently, enhanced I(12,3) clustering detected in Δ (order parameter) *vs.* $1/(T°K)$ plots of native membranes below 28°C (Fig. 6 in Gordon et al. [20]) suggests that the formation of probe-excluding **QCC** tends to segregate I(12,3) in **L**. The nature of this phase separation was further examined with rat liver plasma membranes enriched to a C/P of 0.85 [17]. Such loading decreased the probe concentration at which radical interactions are apparent at 36°C, and this was attributed to the increased formation of cholesterol-rich lipid domains and to the inability of I(12,3) to partition into these domains because of steric hinderance. As the temperature-dependent probe clustering in native membranes may be mimicked isothermally at 36°C, simply by raising the C/P ratio (Fig. 2 in Gordon et al. [17]), we proposed that the **QCC** in native membranes below 28°C are cholesterol-rich domains. Loading to a C/P of 0.85 raised the high onset of the phase separation from 28 to 37°C, as monitored by probe flexibility and clustering. Cholesterol incorporation apparently recruits endogenous phospholipid to create cholesterol-rich **QCC** below 37°C [17]. At physiologic temperatures, cholesterol loading also significantly increases the order parameter of I(12,3)-labeled liver membranes.

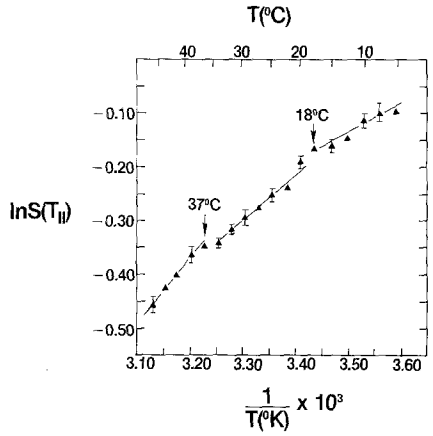

Fig. 4. Arrhenius plot of $S(T_{\parallel})$ for $I(12,3)$-labeled rat liver plasma membranes enriched with cholesterol. $S(T_{\parallel})$ was calculated from Eq. (1) for membranes loaded with 6 μg I(12,3)/mg protein. Results are means ±1 SD for three preparations, with C/P of 0.98, 0.97 and 0.94; the absence of an error bar indicates the SD is less than the symbol size

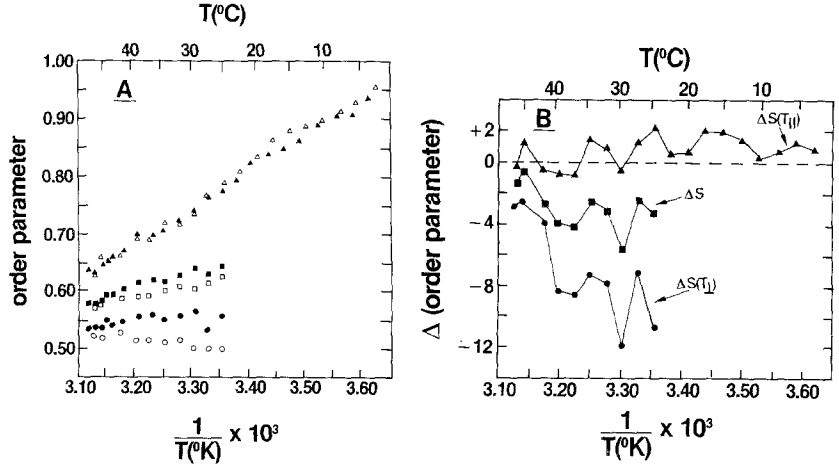

Fig. 5. Temperature dependence of the order parameters of I(12,3)-labeled rat liver plasma membranes enriched with cholesterol [C/P = 0.94]. (*A*): $S(T_{\parallel})$ [▲], S [■] and $S(T_{\perp})$ [●] were measured with a "low" probe concentration (i.e., 2.5 μg probe/mg protein, while $S(T_{\parallel})$ [△], S [□] and $S(T_{\perp})$ [○] were obtained with a "high" probe concentration (i.e., 5 μg probe/mg protein). (*B*): Δ (order parameter) was the percent difference between values measured at the "high" and "low" probe concentrations of *A*

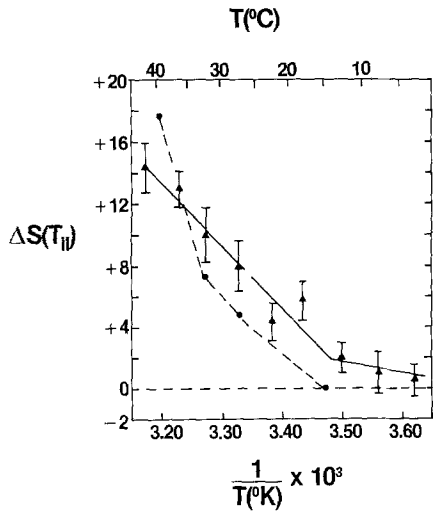

Fig. 6. Effect of cholesterol enrichment on the temperature-dependent fluidity of I(*m*,*n*)-labeled rat liver plasma membranes and human erythrocytes. For rat liver plasma membranes [▲] labeled with 2.5 μg I(12,3)/mg protein, $\Delta S(T_{\parallel})$ is the percent difference between the $S(T_{\parallel})$ measured for cholesterol-enriched rat liver plasma membranes [0.94 ≤ C/P ≤ 0.98] with that of native rat liver plasma membranes [0.60 ≤ C/P ≤ 0.71]; error bars indicate ±1 SEM for four different native and cholesterol-loaded membrane preparations. For I(5,10)-labeled human erythrocytes [●], $\Delta S(T_{\parallel})$ is the percent difference between the $S(T_{\parallel})$ measured for cholesterol-loaded [C/P = 1.90] and native human erythrocyte membranes [C/P = 0.78] (*see* Ref. [42])

The present findings with I(12,3)-labeled rat liver plasma membranes, enriched to C/P of 0.94–0.98, extend these earlier observations. Probe-probe interactions occur at much lower μg probe/mg protein ratios in [C/P = 0.94] membranes than in either native [C/P = 0.71] or [C/P = 0.85] membranes at 36°C (Fig. 5*B*; Fig. 2 of Ref. [17]). Over this C/P range, cholesterol incorporation progressively increases the proportion of cholesterol-rich **QCC** to cholesterol-poor **L**. Moreover, rat liver plasma membranes enriched to a C/P of 0.94 or higher exhibit reduced I(12,3) flexibility at physiologic temperatures: the $S(T_{\parallel})$ for [C/P = 0.94–0.98] membranes is 0.700 at 37°C, while the corresponding $S(T_{\parallel})$ for [C/P = 0.85] or [C/P = 0.71] membranes are 0.670 or 0.580. Interestingly, however, loading to C/P ≥ 0.94 did not substantially alter the onsets of the phase separation over that seen with [C/P = 0.85] membranes (Figs 4,5; Figs. 5*A*,6*A* of Ref. [17]). Although cholesterol-rich and -poor domains exist at physiologic temperatures in both membranes, the inability of loading to C/P of 0.94–0.98 to further elevate the high onset indicates that exogenous cholesterol has only a limited capacity to recruit constituent phospholipid in **QCC**.

Temperature Dependence of Order Parameters and ΔH of I(12,3)-Labeled Native and Cholesterol-Enriched Rat Liver Plasma Membranes

Thermodependent $S(T_{\parallel})$ of native and high-cholesterol liver membranes shows that cholesterol incorporation achieves effects in addition to **QCC** formation at high temperatures (Fig. 6). On heating above 15°C, cholesterol-enriched membranes became increasingly less fluid with respect to native membranes up to 42°C (Fig. 6). Such actions are in accord with the ability of cholesterol, when added to model lipids above their bulk melting temperature, to decrease bilayer fluidity [29]. On the other hand, probe clustering in cholesterol-loaded membranes (Fig. 5*B*) decreases with heating over the same temperature range that cholesterol-enriched membranes become more rigid vis-a-vis native membranes (Fig. 6). This inverse relationship may be due to the disruption of cholesterol-rich **QCC**, which releases sterol into **L** containing probe, thereby reducing I(12,3) flexibility.

It is of interest that the $S(T_{\parallel})$ of native and high-cholesterol liver membranes are similar below 15°C (Fig. 6). Although Schreier et al. [39] emphasized that the order parameter formalism is not strictly applicable for such slow probe motions, $S(T_{\parallel})$ may still be regarded as an empirical parameter sensitive to the polarity and fluidity of the probe environment [7]. Our findings accordingly suggest that I(12,3) samples similar lipid domains in each membrane at low temperatures.

Plots of $\Delta(\Delta H)$ *vs.* $1/T$(°K), where $\Delta(\Delta H)$ is the percent change in ΔH induced by high probe loading, demonstrate that probe-probe interaction effects were much greater at all temperatures for cholesterol-enriched rat liver plasma membranes (*see* Eq. (4) and Fig. 7). As I(12,3) mobility is similar in native and cholesterol-enriched membranes at low temperatures (Fig. 6), enhanced radical interactions in high-cholesterol membranes cannot be simply due to increased probe-probe interactions (i.e., dipole-dipole or spin-exchange) for homogeneously-distributed label. If I(12,3) were to uniformly partition over both native and loaded membranes, then ΔH_{dip} would be identical because of similar probe flexibility at low temperatures (Fig. 6). Similar ΔH_{ex} would also be predicted for probe distributed homogeneously in each system, since probe mobility, and by inference probe diffusion, are equivalent at low temperatures. Since probe-probe interactions are clearly much greater in high-cholesterol membranes, the uniform probe distribution model is unable to account for Fig. 7. The only viable explanation is that I(12,3) sequestration is responsible for

enhanced radical interactions at low temperatures. Consequently, the size of **L** sampled by I(12,3) must be much smaller in cholesterol-loaded membranes. Additional cholesterol/phospholipid adducts formed in high-cholesterol membranes at high temperatures are probably still associated at low temperatures. The smaller size of **L** in cholesterol-enriched membranes is due to phospholipid recruitment by exogenous cholesterol into probe-excluding **QCC**, while the fluidity and polarity of the diminished **L** in cholesterol-loaded membranes remain the same as that of native membranes. A less likely explanation is that cholesterol separates out as a pure phase in either membrane system, or both. Although "pockets" of pure cholesterol would not be expected to significantly perturb the mobility of I(12,3) residing in the **L** of cholesterol-enriched membranes in agreement with Fig. 6, it is difficult to see how such sterol "pockets" would substantially decrease the size of **L**, as is observed in Fig. 7.

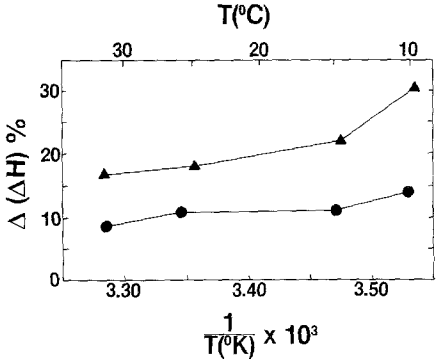

Fig. 7. Effect of cholesterol-enrichment of the $\Delta(\Delta H)$ of I(12,3)-labeled rat liver plasma membranes. For native [C/P = 0.71] liver membranes [●], $\Delta(\Delta H)$ is the percent change of ΔH for membranes labeled with a "high" (27 μg I(12,3)/mg protein) and "low" (2.5 μg I(12,3)/mg protein) probe concentration. For cholesterol-enriched [C/P = 0.85] membranes [▲], $\Delta(\Delta H)$ is the percent change in ΔH for membranes labeled with a "high" (27 μg I(12,3)/mg protein) and "low" (2.5 μg I(12,3)/mg protein) probe concentration

The Thermotropic Lipid Phase Separations in Native and Cholesterol-Enriched Rat Liver Plasma Membranes and Human Erythrocyte Ghosts: Role of Cholesterol

These results allow us to refine an earlier model presented to account for the temperature-dependent lipid phase separation in native rat liver plasma membranes [17, 20]. Above 28°C, bulk lipid is proposed to be homogeneously-distributed as **L**. Below 28°C, cholesterol-rich **QCC** form in a cholesterol-poor liquid lipid matrix (**L'**),

$$\text{Native liver membranes: } \mathbf{L} \xrightarrow[\text{below } 28°C]{T°C \text{ lowered}} \mathbf{L'} + \mathbf{QCC}. \quad [C/P = 0.71]$$

The high temperature break is detected by spin [20, 36] and fluorescence [40] probes, DSC [30] and light scattering [11]. Since no solid or gel phase lipid (**S**) was detected in electron diffraction experiments for temperatures immediately below 28°C [26], we suggested that the fluidity and packing density of **QCC** are in between that of **S** and **L** [20]. Temperature reductions below 28°C progressively increase the ratio of **QCC** to **L'**. It is probable that cooling increasingly depletes **L'** of both cholesterol and lipids reported to have high affinity for cholesterol, such as sphingomyelin and acidic phospholipids [9, 10]. At 18–19°C, a low onset for the phase separation has been noted with spin [20, 36] and fluorescence [30, 40] probes, DSC [30], and electron diffraction experiments on frozen and thawed membranes [26]. In the latter studies, a faint but sharp diffraction ring was observed at a spacing of 4.1 Å (indicating **S**) plus a diffuse band at a spacing of 4.6 Å (indicating **L**). The inability of Hui and Parsons [26] to detect discrete diffraction band(s) arising from **QCC** might be a consequence of obscuring bands due to either the grid holding the membranes or **L** [20]. At 18–19°C, we propose that

$$\text{Native membranes: } \mathbf{QCC} + \mathbf{L'} \xrightarrow[\text{below } 18–19°C]{T°C \text{ lowered}} \mathbf{QCC'} + \mathbf{L''} + \mathbf{S}. \quad [C/P = 0.71]$$

Here, **QCC'** and **L''** are cholesterol-rich and -poor lipid domains below the 18–19°C onset. Although the relative proportion of **S** was not quantitated by Hui and Parsons [26], their diffractographs suggest that **S** constitutes only a small fraction of total lipid. As **S** consists of closely-packed gel lipid, these domains must be cholesterol-free; lipid from either **L'** or **QCC**, or both, may be recruited into **S** below 18°C. Although the 18–19°C transition may signal the end of quasicrystalline cluster formation, we cannot exclude the possibility that the ratio of **QCC'** to **L''** increases somewhat with decreasing temperature.

Cholesterol enrichment profoundly modulates the temperature-dependent lipid phase separation of rat liver plasma membranes. The high temperature onset of **QCC** formation is elevated from 28°C to 37–38°C.

$$\text{High-cholesterol membranes: } \mathbf{L} \xrightarrow[\text{below } 37–38°C]{T°C \text{ lowered}} \mathbf{QCC} + \mathbf{L'}. \quad [C/P \geq 0.85]$$

As before, **QCC** and **L'** are cholesterol-rich and

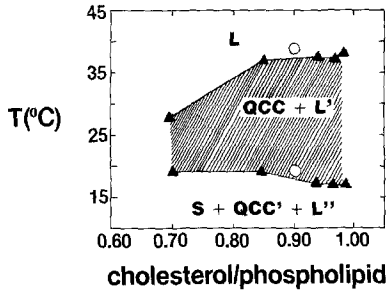

Fig. 8. Effect of cholesterol enrichment on the onset temperatures of the thermotropic lipid phase separation in rat liver plasma membranes. Beginning and ending temperatures for the phase separation in liver membranes (▲) were assigned from Arrhenius plots of order parameters; the high onset was also assigned from Arrhenius-type plots of Δ (order parameters) (*see* Fig. 5*B* and Results and Discussion). Proposed high and low onsets [○] of the thermotropic lipid phase separation of human erythrocyte ghosts are also shown (*see* Results and Discussion for assignments). ***S*** represents close-packed lipid deficient in cholesterol. ***QCC*** and ***QCC'*** reflect "quasi-crystalline" lipid enriched in cholesterol, which tend to exclude I(12,3), and ***L***, ***L'***, ***L''*** represent liquid lipid. The proposed cholesterol concentrations in the liquid lipid domains decrease in the following order: **L** > **L'** > **L''**

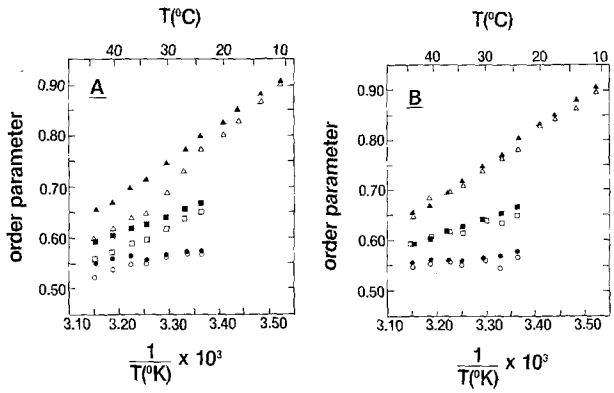

Fig. 9. Temperature dependence of the order parameters of I(12,3)-labeled human erythrocyte ghosts and native [C/P = 0.71] and cholesterol-enriched [C/P = 0.94] rat liver plasma membranes. (*A*): $S(T_{\parallel})$ [▲], $S(T_{\perp})$ [●] and S [■] were determined from erythrocyte ghosts labeled with 15 μg I(12,3)/mg protein, while $S(T_{\parallel})$ [△], $S(T_{\perp})$ [○] and S [□] were obtained from native rat liver plasma membranes [C/P = 0.71] labeled with 2.7 μg I(12,3)/mg protein. (*B*): $S(T_{\parallel})$ [▲], $S(T_{\perp})$ [●] and S [■] were measured from erythrocyte ghosts labeled with 15 μg I(12,3/mg protein, while $S(T_{\parallel})$ [△], $S(T_{\perp})$ [○] and S [□] were obtained from cholesterol-enriched [C/P = 0.94] rat liver plasma membranes labeled with 2.5 μg I(12,3)/mg protein

-poor domains. Cooling increases the proportion of **QCC** to **L'** until the 18–19°C break.

High-cholesterol membranes: **QCC** + **L'** $\xrightarrow[\text{below 18–19°C}]{T\text{°C lowered}}$ **QCC'** + **L''** + **S**(?).
[C/P ≥ 0.85]

QCC'' and **L'** are again defined as cholesterol-rich and -poor lipid domains. It is unknown whether **S** exist in cholesterol-enriched liver plasma membranes, as the necessary electron diffraction experiments have not been performed. For each temperature below 37–38°C, the amount of quasicrystalline cluster lipid in high-cholesterol membranes is greater than that in native membranes, and conversely, the relative amount of **L** is decreased. Some information on the cholesterol content of **L''** is suggested by our finding that cholesterol enrichment does not decrease the fluidity of liver membranes below 15°C (Fig. 6), but rather reduces the size of the liquid lipid pool sampled by I(12,3) (Fig. 7). As electron diffractographs of native membranes show large amounts of **L** below 15°C, cholesterol incorporation into these disordered lipid domains would be expected to decrease the fluidity. Since I(12,3) shows no reduction in flexibility, we propose that **L''** is cholesterol-deficient and that the relative cholesterol concentrations in the liquid lipid domains of either native or high-cholesterol membranes decrease as follows: **L** > **L'** > **L''**.

A phase diagram summarizing the above model for native and cholesterol-modulated rat liver plasma membranes is shown in Fig. 8.

This model accounts for why "breaks" in Arrhenius-type plots of native [17, 36] and cholesterol-enriched (Fig. 4) liver membranes are not as dramatic as thermal profiles of pure lipids undergoing highly cooperative transitions [28]. Here, we postulate that I(12,3) is excluded from both **QCC** and **S**, and formation of domains with low cooperativity exerts only "second-order" perturbations on spin probe mobility. Conversely, Arrhenius-type plots of Δ (order parameters) are exquisitely sensitive to the ratio of **QCC** to **L**, as increases in this ratio greatly enhance probe clustering and radical interactions. Such an assignment is consistent with inhomogeneous distribution of spin probes in mixed lipids of differing fluidities [2].

Spin-label studies on human erythrocyte ghosts [C/P = 0.90] suggest that a thermotropic lipid phase separation occurs involving cholesterol redistribution, analogous to that of cholesterol-enriched rat liver plasma membranes. First, Arrhenius-type plots of Δ (order parameter) indicate that both membranes segregate I(12,3) below 37–38°C (Figs. 3*B* and 5*B*). Second, cholesterol-loading of liver membranes achieves a system which cannot be distinguished from human erythrocyte ghosts, with respect to order parameters over a wide temperature range (Fig. 9*B*); on the other hand, order parame-

ters of native rat liver plasma membranes and human erythrocyte ghosts are very different (Fig. 9*A*). Furthermore, "magnetically-dilute" a_N' for erythrocyte ghosts (15.57 ± 0.05 G) and cholesterol-enriched liver plasma membranes (15.66 ± 0.06 G) are in good agreement at 37°C, while that of native liver membranes is 15.29 ± 0.05 G (errors are SD, with $n = 3$). Cholesterol incorporation increases I(12,3) polarity in liver plasma membranes, such that the polarity of the probe environment becomes identical to that of human erythrocytes. Lastly, cholesterol loading of erythrocyte ghosts labeled with I(5,10) or I(10,3) achieves effects on $S(T_\parallel)$ analogous to those observed with I(12,3)-labeled rat liver plasma membranes (Fig. 6; Refs. [23, 42]). On heating above 15°C, high-cholesterol erythrocyte membranes become increasingly more rigid with respect to native membranes up to 40°C. Cholesterol incorporation may increase the proportion of cholesterol-rich **QCC** at low temperatures; on heating, **QCC** are progressively disrupted and cholesterol is released into **L** sampled by probes.

Remarkably, cholesterol enrichment of rat liver plasma membranes creates an "artificial" system which is degenerate with human erythrocyte ghosts, using such diverse criteria as temperature-dependent I(12,3) clustering and probe flexibility and polarity. Cholesterol content appears to be an important modulator of the thermotropic lipid phase separations in these membranes. Given widely differing protein compositions of erythrocyte and liver membranes, these data also raise the possibility that proteins minimally affect the lipid phase separation. Support for this view comes from DSC studies of lipid-extracts of rat liver plasma membranes, in which protein removal did not disturb the phase separation onsets [30]. Further information on the protein role would likely be provided by ESR experiments on either model lipids mimicking the composition of these membranes or lipid-extracts of erythrocyte and liver membranes.

From the above discussion, a thermotropic lipid phase separation in human erythrocyte ghosts (C/P = 0.90) is tentatively assigned (Fig. 8). The high onset at 37–38°C is detected not only by I(12,3) clustering (Fig. 3*B*) but also by such physical methods as spin probe flexibility [35], fluorescent probe diffusion [14], Raman scattering [45] and DSC [D. Bach, *personal communication*]. We attribute this onset to $\mathbf{L} \rightarrow \mathbf{L}' + \mathbf{QCC}$, where **L** is homogeneously distributed lipid, and **L**′ and **QCC** are cholesterol-depleted and -enriched domains, respectively. Our proposal that cholesterol-rich and -poor domains exist in human erythrocytes is consistent with experiments showing that cholesterol distributes inhomogeneously in this membrane [1, 12, 24]. Of course, additional spin-label studies on cholesterol-manipulated human erythrocyte ghosts will be required to verify this hypothesis. Although a lower limit to the temperature-dependent phase separation was not assessed here using I(12,3), there is evidence for a lipid transition at 10–21°C from a variety of physical-biochemical investigations, including spin [23, 35, 43] and fluorescence [13] probes, light scattering [48], viscosity [47], ^{31}P-NMR [6] positron annihilation [5], Raman scattering [45] and DSC [D. Bach, *personal communication*]. Analogous to cholesterol-loaded rat liver plasma membranes, this transition may correspond to $\mathbf{L}' + \mathbf{QCC} \rightarrow \mathbf{QCC}' + \mathbf{L}''$. As Hui and Strozewski [27] detected **S** in electron diffraction studies of frozen and thawed erythrocyte membranes only at 5°C or less, cholesterol-free **S** apparently does not separate out at the 10–21°C transition.

One criticism of applying the model of Fig. 8 to human erythrocyte ghosts is that no clearly discernible "breaks" occur at characteristic temperatures in Arrhenius-type plots of order parameters. This may be related to I(12,3) exclusion from cholesterol-rich **QCC** and cholesterol-free **S**, and our finding that these domains minimally perturb I(12,3) mobility.

Cold-Induced Hypertonic Lysis (CIHL) of Human Erythrocytes

Intact erythrocytes were exposed to hypertonic medium (0.9 M sucrose) at 37°C for 10 min (Stage 1), and then cooled to 0°C for 10 min (Stage 2). Such treatment achieves pronounced lysis, as assessed by released hemoglobin (Fig. 10). Minimal hemolysis occurred if either Stage 2 was omitted or 0.9 M sucrose was left out of Stage 1 or 2. CIHL was influenced by changing the temperature of Stage 1 from 9 to 46°C. Plots of % hemolysis *vs.* $1/T(°K)$ were approx. sigmoidal, with no significant lysis below 18–20°C and greatest lysis at 40°C. Varying Stage 1 incubation time showed that % lysis increased with time until a plateau was reached at approx. 10 min, for time courses run at 15, 25, 33 and 42°C (data not shown).

The present studies support the data of Green and Jung [22] and their hypothesis that lipid transitions play critical roles in regulating erythrocyte CIHL. The onsets of the phase separation (Fig. 8) are closely correlated with the characteristic temperatures noted in Fig. 10. Here, we suggested that the lipid phase separation in human erythrocytes is due to the formation of cholesterol-rich **QCC** in a cholesterol-poor **L** matrix. It is of some interest then that cooling below 37°C aggregates erythrocyte

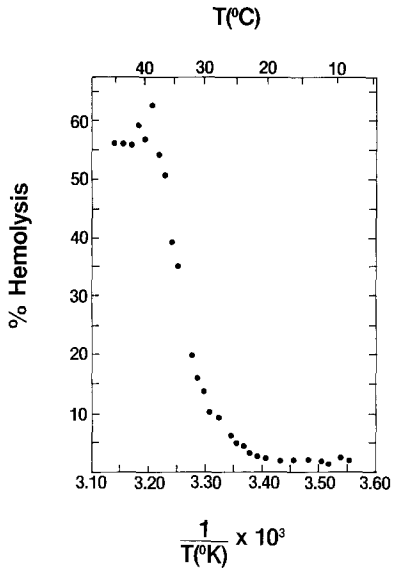

Fig. 10. Temperature dependence of the cold-induced hemolysis of human erythrocytes. Cells were incubated in 0.877 M sucrose for 10 min at 1°C intervals between 9 and 46°C (Step 1) and then subjected to 0°C for 10 min (Step 2). Percent hemolysis was calculated as the fraction of total erythrocyte hemoglobin released after Step 2 (*see* Materials and Methods). Values are means of duplicate determinations

membrane proteins, as assessed by freeze-fracture electronmicroscopy [15, 16] or band 3 rotational mobility [33]. Since integral proteins segregate into cholesterol-poor domains in other membranes [4], we propose that aggregation of erythrocyte proteins at low temperatures is due to selective partitioning into cholesterol-poor **L**. Support for this hypothesis comes from the observation that cholesterol-enrichment of human erythrocyte membranes, an action expected to increase the ratio of **QCC** to **L**, promotes band 3 protein clustering [32]. Also consistent is the finding that slow freezing of erythrocytes releases lipid microvesicles enriched in cholesterol but depleted in intramembrane particles (integral proteins), as determined by freeze-fracture electron microscopy [1]. Formation of cholesterol-rich and -poor domains and sequestering of proteins in cholesterol-poor domains at low temperatures similarly occurs in hypertonic medium, since treatment of erythrocytes with 4 M NaCl at 0 or −11°C releases lipid microvesicles enriched in cholesterol and deficient in protein [1].

The following model is proposed to account for certain aspects of erythrocyte CIHL. Without 0.9 M sucrose, cholesterol-rich and -poor lipid domains form at low temperatures and integral proteins sequester into cholesterol-poor domains. With 0.9 M sucrose, erythrocyte membrane proteins are prevented from normal partitioning, thereby inducing lysis at 0°C. Lateral redistributions of membrane proteins are believed to be crucial in CIHL for several reasons. Although CIHL occurs for cells incubated at 37°C (10 min) and then rapidly cooled to 0°C (10 min), no significant lysis occurs for cells first incubated at 20°C (10 min) and then lowered to 0°C (10 min). Hence, the short-term exposure to approx. 20°C that occurs for cells incubated at 37 and rapidly cooled to 0°C is unable to blunt CIHL, while increasing the incubation time at 20°C to 10 min affords protection. Apparently, the rate-determining step of CIHL Stage 1 exhibits a relatively long (~ min) relaxation time. Since phase separation of lipids between 37 and 20°C will be complete within a few seconds due to rapid diffusion rates, and protein conformation changes are even more rapid, one aspect of CIHL likely to exhibit relaxation times over a period of min is lateral diffusion of integral membrane proteins [28]. The respective actions of hypertonic milieu and the thermotropic lipid phase separation on protein distributions for Stage 1 CIHL are both competitive and kinetically-controlled. This model is consistent with the earlier proposal by Green and Jung [22] that the hypertonic milieu causes membrane-protein damage which prevents normal adjustments to the lipid phase separation.

We thank Mary Wellhoner for technical assistance, and Drs. Cyril C. Curtain and Diane Bach for commenting on the manuscript. This work was sponsored by grants-in-aid from the American Diabetes Association, Southern California Affiliate, Inc., the Kroc Foundation, the Juvenile Diabetes Foundation, the California Metabolic Research Foundation (PWM and LMG) and National Institutes of Health grant HL/AM-27120 (LMG).

References

1. Araki, T. 1979. Release of cholesterol-enriched microvesicles from human erythrocytes caused by hypertonic saline at low temperatures. *FEBS Lett.* **97**:237–240
2. Butler, K.W., Tattrie, N.H., Smith, I.C.P. 1974. The location of spin probes in two phase mixed lipid systems. *Biochim. Biophys. Acta* **363**:351–360
3. Butterfield, D.A., Whisnant, C.C., Chesnut, D.B. 1976. On the use of the spin labeling technique in the study of erythrocyte membranes. *Biochim. Biophys. Acta* **426**:697–702
4. Cherry, R.J., Muller, U., Holenstein, C., Heyn, M.P. 1980. Lateral segregation of proteins induced by cholesterol in bacteriorhodopsin-phospholipid vesicles. *Biochim. Biophys. Acta* **596**:145–151
5. Chow, E.I.-H., Chuang, S.Y., Tseng, P.K. 1981. Detection of a phase transition in red cell membranes using positronium as a probe. *Biochim. Biophys. Acta* **646**:356–359
6. Cullis, P.R., Grathwohl, C. 1977. Hydrocarbon phase transitions and lipid-protein interactions in the erythrocyte membrane. *Biochim. Biophys. Acta* **471**:213–226

7. Curtain, C.C., Gordon, L.M. 1983. Membrane ESR spectroscopy. *In:* Receptor Biochemistry and Methodology. J.C. Venter and L. Harrison, editors. (Vol. 1, Chap. 11) Alan R. Liss, Inc. New York (*in press*)
8. Curtain, C.C., Looney, F.D., Marchalonis, J.J., Raison, J.K. 1978. Changes in lipid ordering and state of aggregation in lymphocyte plasma membranes after exposure to mitogens. *J. Membrane Biol.* **44:**211–232
9. Demel, R.A., Jansen, J.W.C.M., Dijck, P.W.M. van, Deenen, L.L.M. van 1977. The preferential interaction of cholesterol with different classes of phospholipids. *Biochim. Biophys. Acta* **465:**1–10
10. Dijck, P.W.M. van 1979. Negatively-charged phospholipids and their position in the cholesterol affinity sequence. *Biochim. Biophys. Acta* **555:**89–101
11. Dipple, I., Houslay, M.D. 1978. The activity of glucagon-stimulated adenylate cyclase from rat liver plasma membranes is modulated by the fluidity of its lipid environment. *Biochem. J.* **174:**179–190
12. Fisher, K.A. 1976. Analysis of membrane halves: Cholesterol. *Proc. Natl. Acad. Sci. USA* **73:**173–177
13. Flamm, M., Okubo, T., Turro, N.J., Schachter, D. 1982. Pressure dependence of pyrene excimer fluorescence in human erythrocyte membranes. *Biochim. Biophys. Acta* **687:**101–104
14. Galla, H.-J., Luisetti, J. 1980. Lateral and transversal diffusion and phase transitions in erythrocyte membranes. An excimer fluorescence study. *Biochim. Biophys. Acta* **596:**108–117
15. Gerritsen, W.J., Verkleij, A.J., Deenen, L.L.M. van 1979. The lateral distribution of intramembrane particles in the erythrocyte membrane and recombinant vesicles. *Biochim. Biophys. Acta* **555:**26–41
16. Goekoop, J.G., Spies, F., Wisse, D.M., Vries, E. de, Verkleij, A.J., Kempen, G.M.J. van 1980. The appearance of erythrocyte membrane elevations. *Cell Biol. Int. Rep.* **4:**37–42
17. Gordon, L.M., Mobley, P.W., Esgate, J.A., Hofmann, G., Whetton, A.D., Houslay, M.D. 1983. Thermotropic lipid phase separations in human platelet and rat liver plasma membranes. *J. Membrane Biol.* **76:**139–149
18. Gordon, L.M., Sauerheber, R.D. 1982. Calcium and membrane stability. *In:* The Role of Calcium in Biological Systems. L.J. Anghileri and A.-M. Tuffet-Anghileri, editors. Vol. 2, pp. 3–16. CRC Press, Boca Raton
19. Gordon, L.M., Sauerheber, R.D. 1977. Studies on spin-labelled egg lecithin dispersions. *Biochim. Biophys. Acta* **466:**34–43
20. Gordon, L.M., Sauerheber, R.D., Esgate, J.A. 1978. Spin-label studies on rat liver and heart plasma membranes: Effects of temperature, calcium and lanthanum on membrane fluidity. *J. Supramolec. Struct.* **9:**299–326
21. Gordon, L.M., Sauerheber, R.D., Esgate, J.A., Marchmont, R.J., Dipple, I., Houslay, M.D. 1980. The increase in bilayer fluidity of rat liver plasma membranes achieved by the local anesthetic benzyl alcohol affects the activity of intrinsic membrane enzymes. *J. Biol. Chem.* **255:**4519–4527
22. Green, F.A., Jung, C.Y. 1977. Cold-induced hemolysis in a hypertonic milieu. *J. Membrane Biol.* **33:**249–262
23. Herrmann, A., Arnold, K., Lassmann, G., Glaser, R. 1982. Structural transitions of the erythrocyte membrane: An ESR approach. *Acta Biol. Med. Ger.* **41:**289–298
24. Higgins, J.A., Florendo, N.T., Barrnett, R.J. 1973. Localization of cholesterol in membranes of erythrocyte ghosts. *J. Ultrastruct. Res.* **42:**66–81
25. Houslay, M.D., Gordon, L.M. 1983. The activity of adenylate cyclase is regulated by the nature of its lipid environment. *Curr. Top. Membr. Transp.* **18:**179–231
26. Hui, S.W., Parsons, D.F. 1976. Phase transitions of plasma membranes of rat hepatocytes and hepatoma cells by electron diffraction. *Cancer Res.* **36:**1918–1922
27. Hui, S.W., Strozewski, C.M. 1979. Electron diffraction studies of human erythrocyte membranes and its lipid extracts. Effects of hydration, temperature and hydrolysis. *Biochim. Biophys. Acta* **555:**417–425
28. Jain, M.K. 1983. Nonrandom lateral organization in bilayers and biomembranes. *In:* Membrane Fluidity in Biology. R.C. Aloia, editor. Vol. 1, pp. 1–37. Academic, New York
29. Lee, A.G. 1977. Lipid phase transitions and phase diagrams: Mixtures involving lipids. *Biochim. Biophys. Acta* **472:**285–344
30. Livingstone, C.J., Schachter, D. 1980. Lipid dynamics and lipid-protein interactions in rat hepatocyte plasma membranes. *J. Biol. Chem.* **255:**10902–10908
31. Marinetti, G.V., Crain, R.C. 1978. Topology of aminophospholipids in the red cell membrane. *J. Supramol. Struct.* **8:**191–213
32. Muhlebach, T., Cherry, R.J. 1982. Influence of cholesterol on the rotation and self-association of band 3 in the human erythrocyte membrane. *Biochemistry* **21:**4225–4228
33. Nigg, E.A., Cherry, R.J. 1979. Influence of temperature and cholesterol on the rotational diffusion of band 3 in the human erythrocyte membrane. *Biochemistry* **18:**3457–3465
34. Op den Kamp, J.A.F. 1979. Lipid asymmetry in membranes. *Annu. Rev. Biochem.* **48:**47–71
35. Sato, B., Nishikida, K., Samuels, L.T., Tyler, F.H. 1978. Electron spin resonance studies of erythrocytes from patients with Duchenne muscular dystrophy. *J. Clin. Invest.* **61:**251–259
36. Sauerheber, R.D., Gordon, L.M., Crosland, R.D., Kuwahara, M.D. 1977. Spin-label studies on rat liver and heart plasma membranes: Do probe-probe interactions interfere with the measurement of membrane properties? *J. Membrane Biol.* **31:**131–169
37. Sauerheber, R.D., Lewis, U.J., Esgate, J.A., Gordon, L.M. 1980. Effects of calcium, insulin and growth hormone on membrane fluidity. A spin label study of rat adipocyte and human erythrocyte ghosts. *Biochim. Biophys. Acta* **597:**292–304
38. Sauerheber, R.D., Zimmerman, T.S., Esgate, J.A., VanderLaan, W.P., Gordon, L.M. 1980. Effects of calcium, lanthanum and temperature on the fluidity of spin-labeled human platelets. *J. Membrane Biol.* **52:**201–219
39. Schreier, S., Polnaszek, C.F., Smith, I.C.P. 1978. Spin labels in membranes: Problems in practice. *Biochim. Biophys. Acta* **515:**375–436
40. Schroeder, F. 1983. Lipid domains in plasma membranes from rat liver. *Eur. J. Biochem.* **132:**509–516
41. Shukla, S.D., Hanahan, D.J. 1982. Identification of domains of phosphatidylcholine in human erythrocyte plasma membranes. *J. Biol. Chem.* **257:**2908–2911
42. Suda, T., Maeda, N., Shiga, T. 1980. Effects of cholesterol on human erythrocyte membrane. *J. Biochem.* **87:**1703–1713
43. Tanaka, K.-I., Ohnishi, S.-I. 1976. Heterogeneity in the fluidity of intact erythrocyte membranes and its homogenization upon hemolysis. *Biochim. Biophys. Acta* **426:**218–231
44. Verma, S.P., Wallach, D.F.H. 1975. Evidence for constrained lipid mobility in the erythrocyte ghost. A spin-label study. *Biochim. Biophys. Acta* **382:**73–82
45. Wallach, D.F.H., Verma, S.P., Fookson, J. 1979. Applica-

tion of laser Raman and infrared spectroscopy to the analysis of membrane structure. *Biochim. Biophys. Acta* **558:**153–208

46. Whetton, A.D., Gordon, L.M., Houslay, M.D. 1983. Elevated membrane cholesterol concentrations inhibit glucagon-stimulated adenylate cyclase. *Biochem. J.* **210:**437–449
47. Zimmer, G., Schirmer, H. 1974. Viscosity changes of erythrocyte membrane and membrane lipids at transition temperatures. *Biochim. Biophys. Acta* **345:** 314–320
48. Zimmer, G., Schirmer, H., Bastian, P. 1975. Lipid-protein interactions at the erythrocyte membrane. Different influence of glucose and sorbose on membrane lipid transition. *Biochim. Biophys. Acta* **401:**244–255

Received 26 August 1983; revised 7 November 1983